Aerosol Science and Technology
Publication details, including instructions for authors and subscription information:
http://www.tandfonline.com/loi/uast20

Light Scattering Shape Diagnostics for Nano-Agglomerates

George W. Mulholland [a b], Lei Zhou [b], Michael R. Zachariah [a b], William R. Heinson [c], Amit Chakrabarti [c] & Christopher Sorensen [c]

[a] Department of Mechanical Engineering, University of Maryland, College Park, Maryland, USA

[b] Material Measurement Laboratory, National Institute of Standards and Technology, Gaithersburg, Maryland, USA

[c] Department of Physics, Kansas State University, Manhattan, Kansas, USA

Accepted author version posted online: 22 Jan 2013.Version of record first published: 13 Feb 2013.

To cite this article: George W. Mulholland , Lei Zhou , Michael R. Zachariah , William R. Heinson , Amit Chakrabarti & Christopher Sorensen (2013): Light Scattering Shape Diagnostics for Nano-Agglomerates, Aerosol Science and Technology, 47:5, 520-529

To link to this article: http://dx.doi.org/10.1080/02786826.2013.767435

Aerosol Science and Technology, 47:520–529, 2013

ISSN: 0278-6826 print / 1521-7388 online
DOI: 10.1080/02786826.2013.767435

Light Scattering Shape Diagnostics for Nano-Agglomerates

George W. Mulholland,[1,2] Lei Zhou,[2] Michael R. Zachariah,[1,2] William R. Heinson,[3] Amit Chakrabarti,[3] and Christopher Sorensen[3]

[1]*Department of Mechanical Engineering, University of Maryland, College Park, Maryland, USA*
[2]*Material Measurement Laboratory, National Institute of Standards and Technology, Gaithersburg, Maryland, USA*
[3]*Department of Physics, Kansas State University, Manhattan, Kansas, USA*

Motivated by light scattering experiments showing enhanced intensity of electric field aligned nano-agglomerates versus randomly oriented nano-agglomerates, we address the theoretical basis for this effect by applying the theory of small angle Rayleigh-Gans-Debye light scattering to oriented nano-clusters generated by classical diffusion-limited cluster–cluster aggregation (DLCA). We show that the shape anisotropy of these clusters is related to the ratio of small angle light scattering for partially aligned and randomly oriented clusters. It is also shown that state-of-the-art small-angle aerosol scattering measurements would have the angular resolution required to measure the shape anisotropy of clusters with 30 to 1000 nano-monomers. For large q, it is shown from the simulations that $S(q)$ for the partially aligned nano-clusters is not proportional to q^{-D_f}, where D_f is the fractal dimension, as it is for randomly oriented clusters. Nano-clusters with a fixed orientation are shown to result in a structure factor with multiple peaks, which might be used to obtain more detailed information about particle structure than shape anisotropy. The measurements reported in the literature showing enhanced scattering for partially aligned soot agglomerates were for angle integrated measurements. Calculation of the integrated light scattering cross-section for the same range of angles and polarization direction as the experiments indicate a significant enhancement of 70% and 120% for two representative aspect ratios. The smaller value overlaps with measured values of the scattering enhancement for oriented soot agglomerates in an electric field.

INTRODUCTION

Theoretical predictions of light scattering by fractal aerosol nano-agglomerates have focused on the orientationally averaged scattering behavior (Martin and Hurd 1987; Mountain and Mulholland 1988; Sorensen 2001). This is appropriate for most aerosol experiments because the rotation time of the agglomerate is fast compared to the time for the scattering measurement. Even for cases where the measurement is fast, there are typically a large number of agglomerates in the scattering volume each with a random orientation. So, again, the random orientation is a good approximation. The prefix "nano" refers to the monomer particle diameter D being less than about 40 nm or size parameter ($\pi D/\lambda$) less than 0.2, where λ is the wavelength of light.

Such orientationally averaged measurements do not allow the determination of the shape of the agglomerates. There have been measurements of the light scattering by nano-agglomerates, both randomly oriented and partially aligned in an electric field. These measurements have been made for smoke from a variety of fuels, smoke from Kuwait oil fires, and iron oxide chain-aggregates by Chen et al. (1991); Weiss et al. (1992); and Colbeck et al. (1997), respectively. For both of the smoke studies, the authors found that for the fractal agglomerate smoke (soot), the total scattering coefficient increased by 20% to 70% for the aligned soot relative to the randomly oriented soot. For the iron oxide chain aggregates, explicit results for the change in the scattering intensity are not given. However, data from Figure 5 of Chen et al. (1991) for 2.9 μm long chains with 0.06 μm primary sphere diameters indicates a seven fold (700%) increase in the light scattering intensity.

The agglomerates are thought to be aligned with the major axis along the direction of the electric field. Alignment results from the torque acting on the polarizable cluster. Electrical mobility measurements of multiwalled carbon nanotubes (Kim et al. 2009), monodisperse polystyrene sphere doublets (Kousaka et al. 1996; Zelenyuk and Imre 2007), and silver agglomerates (Shin et al. 2010) have demonstrated alignment of these particles in an electric field. The focus of this article is on theoretically demonstrating the feasibility of obtaining shape information for clusters using light scattering measurements on randomly oriented and aligned clusters.

The theory of small angle light scattering (Guinier 1939; Zimm 1948; Tanford 1961; Kerker 1969) relates the orientation

Received 6 October 2012; accepted 26 December 2012.
Address correspondence to George W. Mulholland, Department of Mechanical Engineering, University of Maryland, 2181 Glenn L. Martin Hall, College Park, MD 20742, USA. E-mail: georgewm@umd.edu

averaged light scattering from a particle as a function of scattering angle to the radius of gyration of the particle. Here we extend this analysis to the case of light scattering by a nanocluster aligned along one of its principal axes. The cluster is assumed to be randomly oriented about this axis of rotation. We show how the small angle light scattering intensity, $S(q)$, of the aligned and randomly oriented agglomerate can provide information on the shape of the particle. As will become apparent below, the magnitude of the scattering wave vector, $q = 4\pi \sin\theta/\lambda$, is the more natural variable for describing the light scattering than θ. The key quantity is the slope ratio *SR*, which is equal to the ratio of the slopes of $S^{-1}(\mathrm{q})$ versus q^2 for the oriented agglomerate to the randomly oriented agglomerate. We show how *SR* is related to the anisotropy of the agglomerate. The small angle analysis is also applied to the case of an agglomerate in one fixed orientation.

To assess the feasibility of this approach, diffusion limited cluster–cluster aggregation simulations (DLCA) were carried out producing clusters with sizes up to 1000 monomers. The value of *SR* was computed for these simulated clusters and the relation between *SR* and the shape anisotropy was determined.

The large q behavior for randomly oriented clusters has been widely used to determine the fractal dimension. We have computed the large q behavior to determine whether the fractal dimension can also be determined for clusters aligned along their major axis and for clusters with a fixed orientations. Integrated scattering cross-sections are computed for simulated clusters to provide a qualitative comparison with the enhanced scattering for aligned agglomerates observed by Weiss et al. (1992).

SMALL ANGLE SCATTERING THEORY

Our analysis treats each monomer (or primary sphere) as a point-like scatterer. The scatterers are assumed to be Rayleigh scatterers with the conditions:

$$x = 2\pi a/\lambda \ll 1 \quad |m|\, x = |m|\, 2\pi a/\lambda \ll 1$$

where x is the dimensionless size parameter, λ is the wavelength of light, m is the complex refractive index, and a is the particle radius. The Rayleigh condition ensures a uniform field across the monomer. As discussed below, Rayleigh scattering is a good approximation for $x < 0.2$ for soot-like monomers. The Rayleigh differential scattering cross-section for the monomer for the polarization direction of the incident light perpendicular to the scattering plane is given by (Kerker 1969):

$$\frac{d\sigma^m}{d\Omega} = k^4 a^6 \left|\frac{m^2-1}{m^2+2}\right|^2 . \qquad [1]$$

We assume that the monomers see only the incident light wave and none of the waves scattered by their neighbors; that is, there is no intracluster multiple scattering. The scattered electric field is then the sum of the scattering fields from all the point-like scatterers. This is the Rayleigh-Gans-Debye approximation. The resulting differential scattering cross-section for a cluster with N nano-monomers, $d\sigma^{\mathrm{agg}}(\mathbf{q})/d\Omega$, can be expressed in terms of the Rayleigh scattering cross-section of the monomer and the structure factor, $S(\mathbf{q})$, of the cluster (Mountain and Mulholland 1988; Sorensen 2001):

$$\frac{d\sigma^{\mathrm{agg}}(\mathbf{q})}{d\Omega} = N^2 \frac{d\sigma^m}{d\Omega} S(\mathbf{q}) . \qquad [2]$$

The structure factor $S(\mathbf{q})$ is given by a sum over the N monomers in the agglomerate (Sorensen 2001):

$$S(\mathbf{q}) = \frac{1}{N^2}\left|\sum_{j=1}^{N} e^{-i\mathbf{q}\cdot\mathbf{r}_j}\right|^2 = \frac{1}{N^2}\left[\sum_{j=1}^{N} e^{-i\mathbf{q}\cdot\mathbf{r}_j}\right]\left[\sum_{l=1}^{N} e^{i\mathbf{q}\cdot\mathbf{r}_l}\right] . \qquad [3]$$

The scattering wave vector $\mathbf{q}$ is expressed in terms of the scattered and incident wave vectors, $\mathbf{k_s}$ and $\mathbf{k_i}$.

$$\mathbf{q} = \mathbf{k_s} - \mathbf{k_i} \qquad [4]$$

$$|\mathbf{k}| = k = 2\pi/\lambda \qquad [5]$$

$$|\mathbf{q}| = \frac{4\pi}{\lambda}\sin(\theta/2) \qquad [6]$$

For size parameter $x < 0.2$, it has been found that the above expression for the differential scattering cross-section is accurate to within about 10% for computing the light scattering and absorption for cluster with fractal dimensions of about 1.8 and refractive index of about $1.7 + 0.7\,\mathrm{I}$ (Mulholland et al. 1994). It was also found in this study that for clusters of sizes 17, 52, and 165 monomers, the difference between the predicted radius of gyration based on small angle Rayleigh-Gans-Debye theory and based on the coupled electric and magnetic dipole theory range from 1% to 12% for the same size parameter ($2\pi a/\lambda = 0.15$) as assumed in the current study. Moreover, Wang and Sorensen (2002) experimentally tested the Rayleigh-Gans-Debye theory for a variety of aggregates and found that it worked well within the experimental uncertainties.

We can argue that the light scattering intensity depends on the cluster orientation without computing the intensity. From Equation (3), the angular dependence of light scattering is sensitive only to the scattering particle's dimensions that have components along the scattering wave vector $\mathbf{q}$. In a typical scattering experiment, the scattering wave vector is in the horizontal plane, hence the scattering is dependent only upon an average horizontal extent of the particle. For an ensemble of anisotropic particles, this average horizontal extent or size is larger when the particles have random orientations than that when they are aligned with the major axis perpendicular to the scattering wave vector. Thus, the scattering intensity will be different for the aligned versus unaligned orientation.

Having justified the use of the Rayleigh-Gans-Debye theory for nanocluster, we proceed with deriving the structure factor for

small q. Expanding the exponentials in Equation (3) for small $\mathbf{q}\cdot\mathbf{r_j}$, one obtains the following expression for S($\mathbf{q}$) to order $(\mathbf{q}\cdot\mathbf{r_j})^2$:

$$S(\mathbf{q}) = 1 - \frac{1}{N}\sum_{j=1}^{N}(\mathbf{q}\cdot\mathbf{r_j})^2 + \frac{1}{2N^2}\sum_{j=1}^{N}\mathbf{q}\cdot\mathbf{r_j}\sum_{l=1}^{N}\mathbf{q}\cdot\mathbf{r_l}. \quad [7]$$

The first sum in the last term in Equation (7) can be expressed as:

$$\sum_{j=1}^{N}\mathbf{q}\cdot\mathbf{r_j} = \mathbf{q}\cdot\sum_{j=1}^{N}\mathbf{r_j} = N\mathbf{q}\cdot\mathbf{r_{cm}}. \quad [8]$$

Our coordinate system is defined relative to the center of mass; thus the last term in Equation (7) vanishes so that:

$$S(\mathbf{q}) = 1 - \frac{1}{N}\sum_{j=1}^{N}(\mathbf{q}\cdot\mathbf{r_j})^2. \quad [9]$$

We are interested in the behavior of $S(\mathbf{q})$ for clusters with either a fixed orientation with their long axis perpendicular to the scattering plane, or the same situation but with rotational averaging about the long axis, and finally for a randomly oriented clusters.

The incident light propagates in the z-direction, the polarization and alignment directions are along the x-axis, and the scattering plane is the y-z plane, as shown in Figure 1. For small scattering angles, $\mathbf{q}$ is given by:

$$\begin{aligned}\mathbf{q} &= \frac{4\pi}{\lambda}\sin(\theta/2)\left[-\hat{\mathbf{u}}_\mathbf{z}\sin(\theta/2) + \hat{\mathbf{u}}_\mathbf{y}\cos(\theta/2)\right]\\ &\cong \frac{4\pi}{\lambda}\sin(\theta/2)\,\hat{\mathbf{u}}_\mathbf{y} = q\hat{\mathbf{u}}_\mathbf{y}, \end{aligned} \quad [10]$$

where $\hat{\mathbf{u}}$ represents a unit vector. The component of $\mathbf{q}$ in the x direction is negligible for small θ. Substituting Equation (10) in Equation (9), we obtain:

$$S(q) = 1 - \frac{q^2}{N}\sum_{j=1}^{N}y_j^2 = 1 - q^2Y^2. \quad [11]$$

The quantity Y is the y-component of the radius of gyration, R_g, of the cluster based on the body fixed axis. We shall use the notation S_f to denote the structure factor for a cluster in a fixed orientation. For later reference, we define the quantities X and Z as the other components of R_g.

For the partially aligned case, the x-axis is assumed to be along the major principal axis of the agglomerate. The cluster is aligned but free to rotate about the x-axis. The expression for the aligned structure factor is given by:

$$\langle S(\mathbf{q})\rangle_\alpha = 1 - \frac{1}{N}\sum_{j=1}^{N}\left\langle(\mathbf{q}\cdot\mathbf{r_j})^2\right\rangle_\alpha. \quad [12]$$

The change in coordinates of the monomers resulting from a rotation of angle α about the x-axis is given by:

$$\begin{pmatrix} x_j^r \\ y_j^r \\ z_j^r \end{pmatrix} = \begin{pmatrix} 1 & 0 & 0 \\ 0 & \cos\alpha & \sin\alpha \\ 0 & -\sin\alpha & \cos\alpha \end{pmatrix}\begin{pmatrix} x_j \\ y_j \\ z_j \end{pmatrix}. \quad [13]$$

Using Equations (10) and (13), we obtain the following expression:

$$\mathbf{q}\cdot\mathbf{r_j^r} = q[\cos\alpha y_j + \sin\alpha z_j] \quad [14]$$

Substituting Equation (14) into Equation (12), we obtain:

$$\langle S(q)\rangle_\alpha = 1 - \frac{1}{N}q^2\sum_{j=1}^{N} \times \frac{\int_0^{2\pi}\left[\cos^2\alpha y_j^2 + \sin^2\alpha z_j^2 + 2\sin\alpha\cos\alpha y_j z_j\right]\mathrm{d}\alpha}{\int_0^{2\pi}\mathrm{d}\alpha}. \quad [15]$$

Carrying out the integrations and performing the sum leads to:

$$\langle S(q)\rangle_\alpha = 1 - \frac{1}{2}q^2(Y^2 + Z^2). \quad [16]$$

We shall use the shorthand notation $S_a(q)$ for the structure factor of the partially aligned cluster (rotation about the x-axis). The quantity $\boldsymbol{Z}$ is the z component of the radius of gyration.

The third case is for a random orientation where the agglomerate is rotated through the solid angle 4π. It is convenient to use a coordinate system with $\mathbf{q}$ in the z direction with $\mathbf{r}_\mathrm{j}$ oriented with polar angle θ_1 and azimuthal angle φ_1, where the

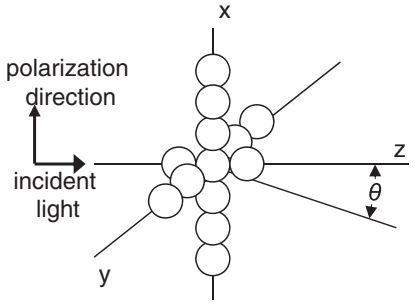

FIG. 1. Schematic of light scattering geometry with the z-y plane—the scattering plane. The orientation of a simple cluster with the major principal axis along the x-direction and the minor principal axis in the z-direction is shown.

subscripts are used to differentiate from the scattering angle θ. The orientation average of the q-r dot product is computed as follows:

$$\left\langle \sum_{j=1}^{N} (\mathbf{q}\cdot\mathbf{r_j})^2 \right\rangle = \sum_{j=1}^{N} q^2 r_j^2 \left\langle \cos^2\theta_{1j} \right\rangle. \quad [17]$$

The orientation average is computed as the integration over θ_1 and φ_1.

$$\left\langle \cos^2\theta_{1j} \right\rangle = \frac{\int_0^{2\pi}\int_0^{\pi} \cos^2\theta_{1j}\sin\theta_{1j}\mathrm{d}\theta_{1j}\mathrm{d}\phi_{1j}}{\int_0^{2\pi}\int_0^{\pi} \sin\theta_{1j}\mathrm{d}\theta_{1j}\mathrm{d}\phi_{1j}} = \frac{1}{3}. \quad [18]$$

From Equations (9), (17), and (18), we find that

$$\langle S(\mathbf{q})\rangle_{\theta_1,\phi_1} = 1 - \frac{q^2}{3N}\sum_{j=1}^{N} r_j^2 = 1 - \frac{1}{3}q^2 R_g^2. \quad [19]$$

In this case, we will use the shorthand notation $S_r(q)$ for the random orientation average.

The key results of this section are Equations (11), (16), and (19). A simple test for the validity of these equations is to consider a spherical particle. In this case, all three equations should give the same result because $X^2 = Y^2 = Z^2$. This is true since $S_f(q)$, $S_a(q)$, and $S_r(q)$ are all equal to $1 - q^2X^2$.

It is noteworthy that one can make a heuristic derivation of the aligned expressions (Equations (11) and (16)) without doing a small q expansion. One notes that $\boldsymbol{q}$ is in the y-direction for small q. So the only length scale appearing in the small q equation for the cluster with a fixed orientation is Y^2. Thus we have the following expression assuming the same general form as for the random orientation:

$$S_r(q) = 1 - cq^2Y^2.$$

However, the constant c must be unity to give the correct result for a spherical particle. For the aligned cluster free to rotate about the x-axis, the length scale in the x-direction does not appear, because $\boldsymbol{q}$ is perpendicular to the x-axis. So, $S_a(q)$ only involves Y^2 and Z^2.

$$S_a(q) = 1 - q^2(c_1Y^2 + c_2Z^2).$$

Again, the coefficients c_1 and c_2 must be one to give the correct result for a spherical particle.

RELATIONSHIP BETWEEN THE SMALL ANGLE STRUCTURE FACTOR AND AGGLOMERATE SHAPE ANISOTROPY

Agglomerate shape is described by the inertia tensor (Fry et al. 2004). For a three-dimensional ($3d$) body of N discrete and equal masses the inertia tensor is

$$T = \sum_{j=1}^{N} \begin{pmatrix} y_j^2 + z_j^2 & -x_j y_j & -x_j z_j \\ -x_j \mathrm{y_j} & x_j^2 + \mathrm{z}_j^2 & -y_j \mathrm{z}_j \\ -x_j z_j & -y_j z_j & x_j^2 + y_j^2 \end{pmatrix}. \quad [20]$$

Diagonalizing T and dividing by the number of monomers N, one obtains the square of principal radii of gyration R_j^2 for $j = 1, 2, 3$ with $R_1 \le R_2 \le R_3$. Anisotropy is used as a measure of cluster "stringiness" and can be defined by the ratio of the squares of principal radii of gyration (Fry et al. 2004):

$$A_{ij} = \frac{R_i^2}{R_j^2} \quad [21]$$

where $i, j = 1, 2, 3$. Here we focus on the ratio A_{31}, which is the ratio of the largest to the smallest principal radii of gyration. The radius of gyration R_g is used as a measure of the overall cluster size, which is related to the principal radii of gyration R_i^2 in the following way:

$$R_g^2 = \frac{1}{2}\left(R_1^2 + R_2^2 + R_3^2\right). \quad [22]$$

Here we define another measure of shape anisotropy the slope ratio, SR, which is the ratio of slopes of $S(q)^{-1}$ versus q^2 for the random orientation (Equation (19)) to the partially aligned orientation (Equation (16)).

$$SR = \frac{2}{3}\frac{(X^2 + Y^2 + Z^2)}{(Z^2 + Y^2)} = \frac{2}{3}\frac{R_g^2}{(Z^2 + Y^2)}. \quad [23]$$

From the definitions of X, Y, and Z below Equation (11) and the definitions of the principal radii of gyration, one finds the following relationships between R_1, R_2, and R_3 and X,Y, and Z:

$$R_1^2 = Y^2 + Z^2, \quad [24]$$
$$R_2^2 = Z^2 + X^2, \quad [25]$$
$$R_3^2 = Y^2 + X^2. \quad [26]$$

Note that the body fixed axis is aligned in the direction of the principal axes with the x-axis in the direction of the principal axis and the z-axis in the direction of the minor axis.

From these three equations together with the definitions of SR and A_{31}, one obtains the following relationship:

$$SR = \frac{2}{3}\left(A_{31} + \frac{Z^2}{Z^2 + Y^2}\right). \quad [27]$$

The quantity A_{31} is always greater than 1 while the 2nd term is always smaller than 0.5 because Z is the smallest component of the radius of gyration. In a later section, we will analyze the

correlation between SR and A_{31} for clusters ranging in size from 10 to 1000 monomers.

SIMULATION

Clusters used in this work were obtained from an off-lattice diffusion limited cluster aggregation (DLCA) algorithm (Fry et al. 2004) using an efficient link-list method (Allen and Tildesly 1987). DLCA simulations successfully model aggregates formed in aerosols and colloids which yield $D_f = 1.8$ (Family and Landau 1984; Jullien and Botet 1987; Meakin 1999). These simulations started with 10^6 particles at a monomer volume fraction of $f_v = 0.001$ that were randomly placed in a three-dimensional box. At the beginning of each time step, the number of clusters N_c was counted (note that the number of monomers was included in N_c). A random cluster was chosen and time was incremented by N_c^{-1}. The probability that the cluster moved was inversely proportional to that cluster's radius of gyration ($p \propto R_g^{-1}$) and was normalized so that monomers had $p = 1$. Clusters moved in random directions a distance of one monomer diameter. When two clusters collided, they irreversibly stuck together, and N_c was decremented by 1. The resulting cluster sizes ranged from a few monomers to more than 1000. Rotational motions of the clusters were neglected in these simulations.

The output of the simulations includes the coordinates of each monomer in the cluster. The inertia tensor, Equation (20), was diagonalized for each cluster giving the principal radii (eigenvalues) and their orientation (eigenvectors) relative to the space fixed coordinate system. For each cluster the radius of gyration R_g, the anisotropy A_{31}, and the slope ratio SR are computed from the principal radii of gyration using Equations (21) to (26).

The structure factor is computed for a scattering geometry illustrated in Figure 1. The incident light with an assumed wavelength of 405 nm is propagating in the z direction and is linearly polarized in the x direction. The monomer size parameter, $2\pi a/\lambda$, based on a 10 nm momomer radius is 0.155. This value of the size parameter is typical for light scattering measurements for soot. The assumed monomer size and wavelength are typical of the conditions for light scattering measurements of soot though larger monomer sizes and wavelengths are also common. The scattering plane is the y-z plane with scattering angle θ. The clusters are oriented with the major axis, R_3, in the x direction and the minor axes R_1 is aligned in the z direction. The orientation is shown for an idealized cluster in Figure 1. Based on the monomer coordinate location relative to the principal axis coordinate system with origin at the center of mass, the structure factor is computed using Equation (3) and (6) as a function of q for angles ranging from 0° to 180°. For the partially aligned orientation, the value of $S(q)$ is computed with rotations every 10° as the cluster is rotated about the z-axis. The average of these values is denoted as $S_a(q)$. The random orientation average is obtained by computing $S(q)$ for 216 orientations covering the full range of Euler angles for the coordinate axes for a fixed scattering angle. The average of these values is denoted as $S_r(q)$.

RESULTS

Small q Behavior of Structure Factor

The small q results are expressed as $1/S(q)$, which is the Zimm plot formalism and has been widely used for fractal aerosol agglomerates (Sorensen 2001). For small q, the asymptotic expression based on Equations (16) and (19) are:

$$1/S_a(q) = 1 + \frac{1}{2}q^2(Z^2 + Y^2), \quad [28]$$

$$1/S_r(q) = 1 + \frac{1}{3}q^2R_g^2. \quad [29]$$

A key issue in analyzing the results is the range of q over which the computed $S(q)$ is described by the above equation. This is important in assessing the feasibility of quantitatively determining SR defined by Equation (23) by light scattering experiments.

The structure factors were computed for clusters with nominally 30 spheres, 100 spheres, 300 spheres, and 1000 spheres generated by the DLCA described above. Five clusters were selected for each of these cluster sizes, with A_{31} ranging from about 2 to 6. The x-z projected image of 300 sphere clusters, with A_{31} equal to 2 and 6 are shown in Figure 2 to illustrate the range of aspect ratios considered in this study. For the 300

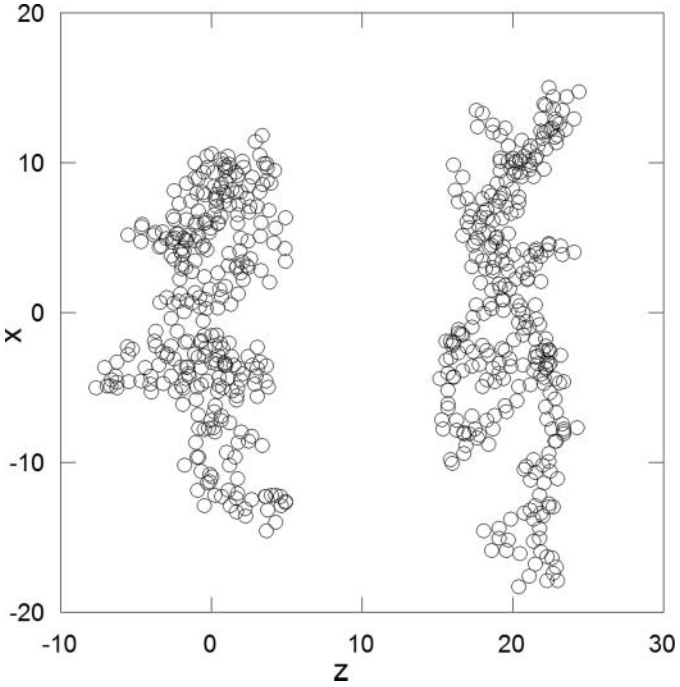

FIG. 2. x-z projection of 300 sphere clusters with $A_{31} = 2.13$ (left) and 6.07 (right).

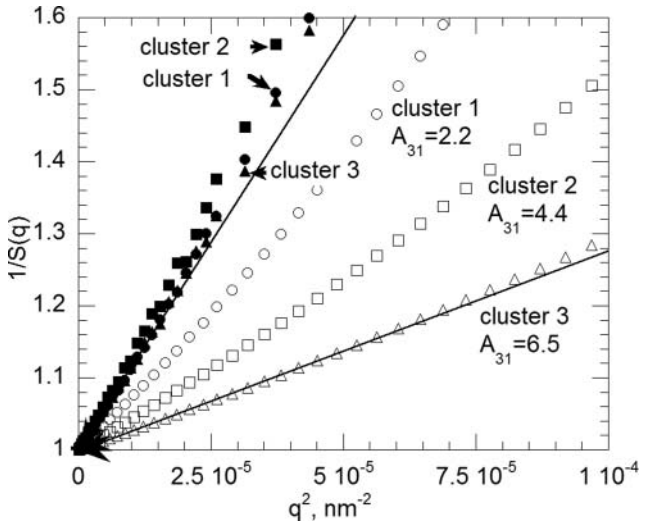

FIG. 3. Effect of shape on $1/S(q)$ for 300 sphere nano-clusters, $A_{31} = 2.18$ cluster 1, $A_{31} = 4.35$ cluster 2, $A_{31} = 6.54$ cluster 3. Open symbols refer to partially aligned particles and the solid to the randomly oriented. The solid lines are visual fits for values of $1/S(q)$ less than 1.2.

sphere clusters, the average value of A_{31} is about 4.0 and the standard deviation is about 2.0. This range contains a majority of the clusters, though the population is broad with 3 of the 137 clusters with values of A_{31} larger than 10.

The effect of alignment on $1/S(q)$ is shown for the 300 sphere clusters in Figure 3. It is seen that the Zimm-type plots give a linear dependence of $1/S(q)$ on q^2 as predicted by Equations (28) and (29). This plot shows that the partially aligned scattering is correlated with the anisotropy A_{31} with the slope decreasing by about a factor of 3 for particle 3 relative to particle 1 as A_{31} increases by about a factor of 3. It is also apparent from Figure 3 that there is a much smaller variation in the slope for the random orientation as A_{31} is changed.

A closer inspection indicates that there is a slight upward curvature in the plots. This is evident from the deviation between the calculated points and the visual linear fit to the data for particle 3 for $1/S(q) < 1.2$. The slope ratio *SR*, defined by Equation (23), is equal to the ratio of the slope for the randomly oriented cluster to the aligned cluster in the limit as q approaches zero. Of course, such a limit cannot be reached experimentally. We have simulated possible experimental observation by making visual linear fits to the random and aligned orientations and then computing the ratio. We find that *SR* computed from the visual fits agrees within 3% with the exact value of *SR* computed using the coordinates of the cluster (Equation (23)) for the three clusters shown in Figure 3. Table 1 compares the visual fit with the exact results for 10 different clusters, ranging in size from 30 monomer to 1000 monomers, and the largest discrepancy is 6%. This demonstrates the potential for obtaining shape information from precise small angle scattering measurements for aligned and randomly oriented clusters. As the cluster size increases, the range of q for linear $1/S(q)$ versus q^2 decreases. For random

TABLE 1
Comparison of *SR* based on cluster coordinates and *SR* from small q fit of $1/S(q)$ for clusters generated by DLCA

N	Rg, nm	A_{31}	*SR* (Equation (23))	*SR*(fit)	% diff[a]
31	50.1	2.18	1.63	1.59	−2.8
30	63.2	4.35	3.01	2.96	−1.6
30	71.9	6.54	4.60	4.47	−2.9
307	180	2.13	1.54	1.56	0.9
301	192	3.93	2.89	2.87	−0.5
304	183	6.07	4.30	4.17	−3.1
100	92	2.06	1.67	1.57	−6.0
100	128	3.86	2.67	2.63	−1.5
1007	337	2.08	1.53	1.51	−1.6
989	369	4.10	2.99	3.04	1.8

[a]% diff $= \frac{SR(\text{fit}) - SR(\text{Eq23})}{SR(\text{Eq23})} 100$

orientation, the range of q decreases about six-fold from 1.2×10^{-2} nm^{-1} to 2×10^{-3} nm^{-1} as the cluster size increases from 30 monomers to 1000 monomers. The angle range for all the computed values of $S(q)$ corresponding to a 20% increase in $1/S(q)$ is 7° to 83°. Estimating *SR* from experimental data would require at least three points distributed uniformly with regard to q^2. This would require forward scattering measurements at angles as small as about 2°.

The above analysis demonstrates that the asymmetry of model clusters aligned in an electric field can be measured by small angle light scattering. The uncertainty in the experimental determination of *SR* will be affected by the angular resolution for small angles, the noise/drift in the intensity, and the other common problems of stray light and sensitivity in light scattering measurements. Two other issues regarding the real clusters are the degree of alignment in the electric field and the polydispersity of the cluster size and aspect ratio.

The correlation between *SR* and A_{31} was studied by plotting *SR* versus A_{31} for a total of 227 clusters with 30 monomers and for 137 clusters with 300 monomers generated by DLCA. A good correlation is evident from Figure 4. Linear regression leads to slopes that agree within 1%:

$$SR = 0.166 + 0.671 A_{31},$$
$$\mathrm{R} = 0.9992 \text{ for 30 monomer clusters;} \quad [30]$$
$$SR = 0.161 + 0.675 A_{31},$$
$$\mathrm{R} = 0.9988 \text{ for 300 monomer clusters.} \quad [31]$$

The deltas between the value of *SR* from the cluster coordinates and the regression line given by Equation (31) are randomly distributed about zero and the standard deviation of the deltas is 0.062. These regression lines underestimate the limiting value of $SR = 1$ for $A_{31} = 1$. It was expected that a bias would be evident for small values of A_{31}; however, we

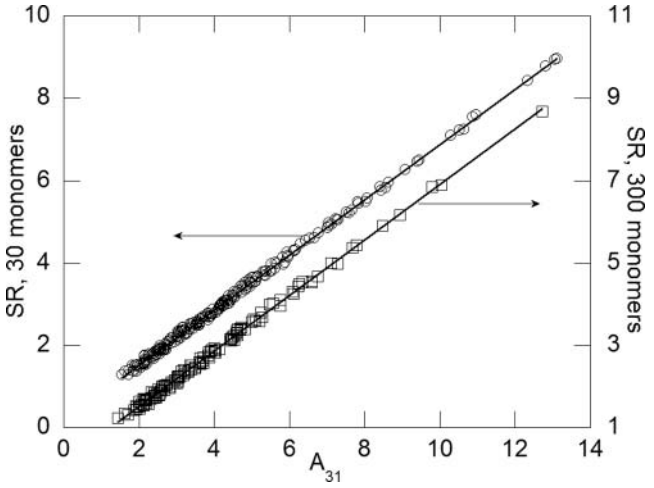

FIG. 4. Linear regression of *SR* versus anisotropy for 227 clusters with 30 monomers and 137 clusters with 300 monomer produced by DLCA. The axis is offset on the right hand side to allow viewing of both correlation lines. The mean and standard deviation for *SR* and A_{31} are 3.11 ± 1.52 and 4.38 ± 2.27 for 30 monomer clusters and 2.82 ± 1.53 and 3.94 ± 2.27 for the 300 monomer clusters.

see only a hint of a bias in the deviation plot for the smallest values.

The regression expressions are consistent with Equation (27). The slopes are within 1% of the slope in Equation (27). The second term in Equation (27) can vary at most from a value of 0 ($Z = 0$) and 0.333 ($Z = Y$). The average of these two values is within 4% of the two regression intercepts.

Large *q* Behavior of Structure Factor

The large q behavior of the structure factor is widely used for determining the fractal dimension of nano-agglomerates both as aerosols and as colloidal suspensions. The results of many of these studies are summarized by Sorensen (2001). The large q behavior is shown in Figure 5 for four clusters with sizes ranging from 30 monomers to 1000 monomers. The clusters were selected so that the anisotropy, A_{31}, for each cluster was close to 4.0. For large q, the structure factors for the randomly oriented 300 and 1000 monomer cluster have a linear dependence on q for the log–log plot with a slope of about -1.8. This is a characteristic value seen in simulations and experimentally for diffusion limited cluster–cluster aggregation as discussed by Sorensen (2001). It is noteworthy that the aligned nano-agglomerates do not show this behavior. For the 1000 sphere cluster, there is a reasonably constant slope of about -3.2 for q between 0.01 nm^{-1} and 0.02 nm^{-1}, but then $S(q)$ becomes nearly constant as q approaches 0.03 nm^{-1}. For the 300 monomer cluster $S(q)$ has a bowed appearance with a slope of about -3.0 for q in the range 0.02 nm^{-1} to 0.03 nm^{-1}.

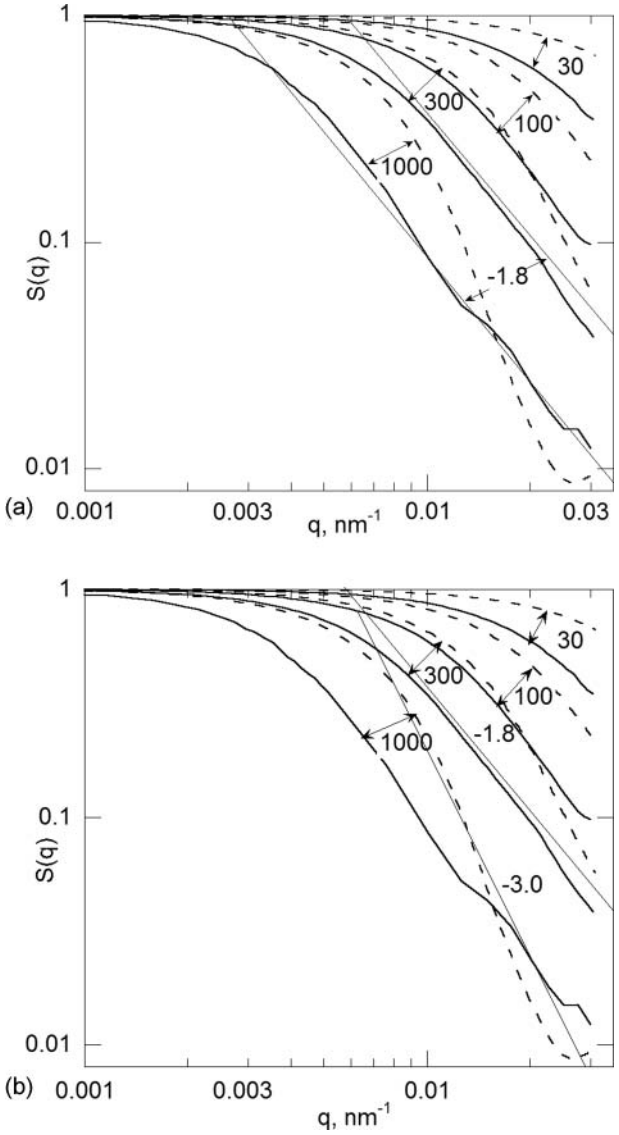

FIG. 5. The effect of the number of monomers in the cluster on the structure factor for a wide range in q. The value of A_{31} in all four cases is near 4.0. The solid lines correspond to a random orientation and the dashed lines to a partially aligned orientation. One faint line is drawn with a slope of -1.8, which is close to the fractal dimension of the cluster. A second faint line with a slope of -3 is drawn to help show the qualitative difference between the randomly oriented structure factor and that for the aligned clusters.

COMPARISON WITH EXPERIMENT/POTENTIAL APPLICATION

Currently there are no experimental data to compare our results for small angle measurements of aligned versus random nano-agglomerates. However, Weiss et al. (1992) and Colbeck et al. (1997) have measured integrated light scattering from soot agglomerates in a random orientation and then in a partially aligned position with an electric field applied. The light scattering measurement was made with a reciprocal nephelometer

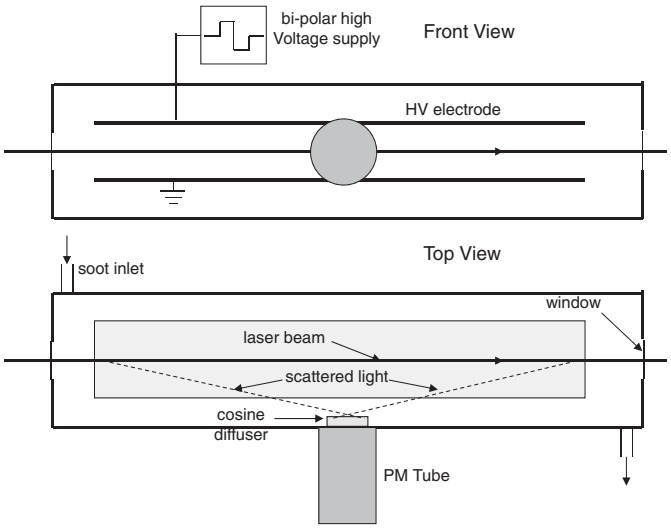

FIG. 6. Schematic of a reciprocal nephelometer with inserted electrodes for orienting the agglomerates. The scattered light is collected by the cosine diffuser over an angle range of about 7° to 173°. The shaded section in the top view represents the electrode.

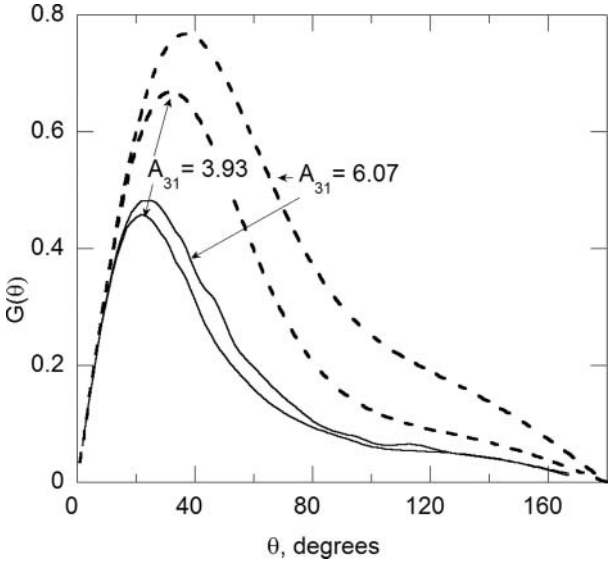

FIG. 7. The angular dependence of the combined angular function for the partially aligned 300 monomer nano-cluster shown by dashed curves and the random oriented nano-cluster shown by the solid line. For each orientation, results are given for two values of the anisotropy A_{31}.

(Figure 6), which collects scattered light from 7° to 173° with a cosine diffuser. A pair of electrodes was positioned in the center of the cell to align the soot. In one experiment (Weiss et al. 1992), a square wave electric field of ± 2kV cm^{-1} was applied to the plates for 2 ms at 12.5 Hz. Both studies referenced above found an enhancement of 20% to 70% when the soot is aligned with the electric field on.

It is of interest to compute the enhancement for the simulated soot. In both cases, the investigators used a reciprocal type nephelometer where a cosine sensor/PM tube oriented normal to the laser beam collects scattered light from about 7° to 173°. For this geometry, the integrated scattering cross-section is related to scattering cross-section given in Equation (2) (Mulholland and Bryner 1994):

$$C'_{\mathrm{sca},a} = \int_{7^\circ}^{173^\circ} \left\langle \frac{d\sigma^{\mathrm{agg}}(q)}{d\Omega} \right\rangle_a \sin\theta \mathrm{d}\theta, \qquad [32]$$

where

$$\left\langle \frac{d\sigma^{\mathrm{agg}}(\mathbf{q})}{d\Omega} \right\rangle_a = N^2 \frac{d\sigma^m}{d\Omega} S_a(q) \frac{1}{2}(1+\cos^2\theta). \qquad [33]$$

The prime is used to distinguish this cross-section from the total scattering cross-section. The subscript a refers to the partially aligned orientation and there is a parallel expression with subscript r for the random orientation. The term $1/2(1+\cos^2\theta)$ accounts for the Rayleigh scattering for the randomly polarized light source thought to be used in the experiments. This term was not included in our previous analysis, since the polarization direction was perpendicular to the scattering plane. The scattering cross-section can be expressed as a product of the integral of a combined angular function $G_a(\theta)$ and an angle independent term denoted as A.

$$C'_{\mathrm{sca},a} = \mathrm{A} \int_{7^\circ}^{173^\circ} G_a(\theta) d\theta, \qquad [34]$$

where

$$G_a(\theta) = \left(1+\cos^2\theta\right) \sin\theta S_a(\theta) \qquad [35]$$

and

$$A = \frac{1}{2} N^2 \frac{d\sigma_m}{d\Omega}. \qquad [36]$$

Angular average scattering cross-sections were computed for 300 sphere nano-agglomerates with A_{31} equal 3.93, nearly the average value for 137 clusters, and A_{31} equal 6.07, close to the sum of the average value plus the standard deviation. The monomer size parameter was the same as for the previous calculations ($\pi \mathrm{D}/\lambda = 0.155$). The peak in the combined angular function is larger for the partially aligned clusters compared to the randomly oriented clusters as indicated in Figure 7. The ratio of $C'_{\mathrm{sca},a}/C'_{\mathrm{sca},r}$ is 1.76 for A_{31} equal 3.93 and is 2.20 for A_{31} equal 6.07. This increase in the ratio with increasing A_{31} is the same trend as for the slope ratio *SR*. However, the integral in Equation (32) is not related to A_{31} in a straightforward manner. The observed ratio of cross-sections (Weiss et al. 1992; Colbeck et al. 1997) is in the range of 1.2 to 1.7.

The measured values are mostly less than either of our estimated values. One reason relates to the simulation parameters. Our simulation is based on nano-clusters with 300 monomers.

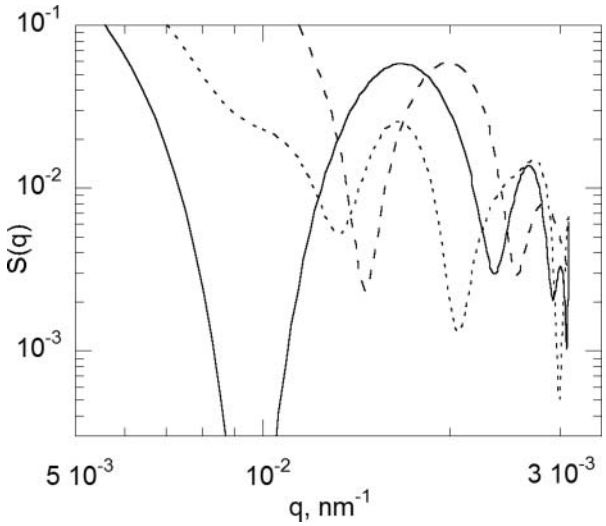

FIG. 8. S(q) is plotted for a nano-cluster with 1007 monomers. Each curve corresponds to a different orientation of the cluster. The solid curve corresponds to the largest principal axes in the y-direction, the short dashed curve for largest principal axis in the z-direction, and the long dashed curve for largest principal axis in the x-direction. In all three cases, the light is propagating in the z-direction and polarized in the x-direction with the y-z plane—the scatter plane.

For the experimental conditions, there is likely a broad distribution of clusters extending to more than 1000 monomers. There is also the possibility that the principal axis of the cluster is not fully aligned in the direction of the electric field.

An existing light scattering instrument (Dick 2006) is capable of measuring $S(q)$ at 12 polar angles for a single particle over a time small compared to the rotation time interval of about 3 μs. This time is of 1–5 ms for the smoke agglomerates studied by Colbeck et al. (1997) and Weiss et al. (1992). If a single cluster were trapped at a fixed location, then A_{31} could be determined from a series of measurements of $S(q)$ as the cluster rotates using an instrument such as Dick's. The ratio of the average slope (random orientation) to the minimum slope of $S(q)^{-1}$ versus q^2 would be equal to A_{31}. The large q behavior of $S(q)$ for a fixed orientation shown in Figure 8 has multiple peaks and likely contains more information about the particle structure than A_{31}. These features arise from constructive and destructive interference from the scattered waves. For example, the first minimum shown in Figure 8 occurs for the major principal axis aligned with the y-axis, since the phase shift is approximately proportional to the y component of the radius of gyration (Equation (11)). The orientation averaging (Figure 6) removes these diffraction peaks.

CONCLUSIONS

A theory has been developed for computing the small angle light scattering by nano-clusters with fixed orientation and for nano-clusters aligned along their major principal axis. The ratio of the small angle slope for 1/S(q) versus q^2, *SR,* is shown to be related to the principal components of the inertia matrix. The values of *SR* were obtained from linear fits of Zimm plots for DLCA clusters in a process similar to what would be done experimentally. The resulting value of *SR* was within 5% of the predicted asymptotic small angle value. It is also shown that *SR* is well correlated with the ratio of the squares of the principal radii of gyration, A_{31}. For *SR* over the range of 1.5 to 9, the standard deviation from the regression line is $\pm$ 0.06. This demonstrates the possibility of determining the shape of agglomerates by making small angle light scattering measurements for partially aligned and randomly oriented agglomerates.

For large q for nano-clusters with 30, 100, 300, and 1000 monomers, it is shown from the simulations that $S(q)$ for the partially aligned clusters is not proportional to q^{-D_f} as it is for the randomly oriented clusters. Nano-clusters with a fixed orientation are shown to produce diffraction peaks. Calculation of the integrated light scattering cross-sections for 300 sphere nano-clusters indicate a significant increase of 70% and 120% for partially aligned versus randomly oriented clusters for two representative aspect ratios. The smaller value overlaps with measured values of the scattering enhancement for oriented soot agglomerates in an electric field (Weiss et al. 1992; Colbeck et al. 1997).

REFERENCES

Allen, M., and Tildesly, D. (1987). *Computer Simulation of Liquids*. Clarendon Press, Oxford.

Chen, M. T., Xie, G. W., Yang M., and Shaw D. T. (1991). Experimental Characterization of Chain-Aggregate Aerosol by Electrooptic Scattering. *Aerosol Sci. Technol.*, 14:74–81.

Colbeck, I., Atkinson, B., and Johart Y. (1997). The Morphology and Optical Properties of Soot Produced by Different Fuels. *J. Aerosol Sci.*, 28:715–723.

Dick, W. D. (2006). *Internal Report by MSP Corp on Multi-Angle Light Scattering Photometer*, Shoreview, MN, USA.

Family, F., and Landau, D. P. (eds.) (1984). *Kinetics of Aggregation, and Gelation*. North Holland, and Elsevier, Amsterdam.

Fry, D., Mohammad, A., Chakrabarti, A., and Sorensen, C. M. (2004). Cluster Shape Anisotropy in Irreversibly Aggregating Particulate Systems. *Langmuir*, 20:7871.

Guinier, A. (1939). La Diffraction Des Rayons X Aux Trespetits Angles: Application a L'etude de Phenomes Ultramicroscopiques, [The Diffraction of X-Rays at Very Small Angles: Application to the Study of Ultramicroscopic Phenomena.] *Ann. Phys.*, 12:161–237.

Jullien, R., and Botet, R. (1987). *Aggregation, and Fractal Aggregates*, World Scientific, Hackensack, New Jersey.

Kerker, M. (1969). *The Scattering of Light and Other Electromagnetic Radiation*, Academic, New York.

Kim, S. H., Mulholland, G. W., and Zachariah, M. R. (2009). Density Measurement of Size Selected Multiwalled Carbon Nanotubes by Mobility-Mass Characterization, *Carbon*, 47:1297–1302.

Kousaka, Y., Endo, Y., Ichitsubo, H., and Alonso, M. (1996). Orientation-Specific Dynamic Shape Factors for Doublets and Triplets of Spheres in the Transition Regime. *Aerosol Sci. Tech.*, 24:36–44.

Martin, J. E., and Hurd, A. J. (1987). Scattering from Fractals. *J. Appl. Cryst.*, 20:61–78.

Meakin, P. (1999). A Historical Introduction to Computer Models for Fractal Aggregates. *J. Sol. Gel. Sci. Technol.*, 15:97.

Mountain, R. D., and Mulholland, G. W. (1988). Light Scattering from Simulated Smoke Agglomerates. *Langmuir*, 4:1321.

Mulholland, G. W., Bohren, C. F., Fuller, K. A. (1994). Light Scattering by Agglomerates: Coupled Electric and Magnetic Dipole Method. *Langmuir*, 10:2533–2546.

Mulholland, G. W., and Bryner, N. P. (1994). Radiometric Model of the Transmission Cell-Reciprocal Nephelometer. *Atmos. Environ.*, 28: 873–887.

Shin, W. G., Mulholland, G. W., and Pui, D. Y. H. (2010). Determination of Volume, Scaling Exponents, and Particle Alignment of Nanoparticle Agglomerates Using Tandem Differential Mobility Analyzers. *J. Aerosol. Sci.*, 41:665–681.

Sorensen, C. M. (2001). Light Scattering by Fractal Aggregates: A Review. *Aerosol Sci. Technol.*, 35:648–687.

Tanford, C. (1961). *Physical Chemistry of Macromolecules*, Wiley, New York.

Wang, G. M., and Sorensen C. M. (2002). Experimental Test of the Rayleigh-Gans-Debye Theory for Light Scattering by Fractal Aggregates. *Appl. Opt.*, 41:4645–4651.

Weiss, R. E., Kapustin, V. N., and Hobbs, P. V. (1992). Chain-Aggregate Aerosols in Smoke from the Kuwait Oil Fires. *J. Geophys. Res.*, 97:14,527–14,531.

Zelenyuk, A., and Imre, D. (2007). On the Effect of Particle Alignment in the DMA. *Aerosol Sci. Technol.,* 41:112–124.

Zimm, B. H. (1948). Apparatus and Methods for Measurement and Interpretation of the Angular Variation of Light-Scattering, Preliminary Results on Polystyrene Solutions. *J. Chem. Phys.*, 16:1099–1116.